Compound I in Heme Thiolate Enzymes: A Comparative QM/MM Study†

Kyung-Bin Cho,‡ Hajime Hirao,‡ Hui Chen,‡ Maria Angels Carvajal,‡ Shimrit Cohen,‡ Etienne Derat,‡,§ Walter Thiel,|| and Sason Shaik*,‡

Department of Organic Chemistry and The Lise Meitner-Minerva Center for Computational Quantum Chemistry, The Hebrew University of Jerusalem, 91904 Jerusalem, Israel, and Max-Planck-Institut für Kohlenforschung, Kaiser-Wilhelm-Platz 1, 45470 Mülheim an der Ruhr, Germany

Received: July 30, 2008

This study directly compares the active species of heme enzymes, so-called Compound I (Cpd I), *across the heme-thiolate enzyme family*. Thus, sixty-four different Cpd I structures are calculated by hybrid quantum mechanical/molecular mechanical (QM/MM) methods using four different cysteine-ligated heme enzymes ($P450_{cam}$, the mutant $P450_{cam}$-L358P, CPO and NOS) with varying QM region sizes in two multiplicities each. The overall result is that these Cpd I species are similar to each other with regard to many characteristic features. Hence, using the more stable CPO Cpd I as a model for P450 Cpd I in experiments should be a reasonable approach. However, systematic differences were also observed, and it is shown that NOS stands out in most comparisons. By analyzing the electrical field generated by the enzyme on the QM region, one can see that (a) the protein exerts a large influence and modifies all the Cpd I species compared with the gas-phase situation and (b) in NOS this field is approximately planar to the heme plane, whereas it is approximately perpendicular in the other enzymes, explaining the deviating results on NOS. The calculations on the $P450_{cam}$ mutant L358P show that the effects of removing the hydrogen bond between the heme sulfur and L358 are small at the Cpd I stage. Finally, Mössbauer parameters are calculated for the different Cpd I species, enabling future comparisons with experiments. These results are discussed in the broader context of recent findings of Cpd I species that exhibit large variations in the electronic structure due to the presence of the substrate.

Introduction

Heme proteins are an important class of proteins responsible for a variety of functions in the nature. Of particular interest in many of their reactions is the elusive Por(+•)Fe(IV)═O intermediate, so-called Compound I (Cpd I), which is considered to be the active species of these enzymes. The first report about this species was published in 1941 when it was observed in horseradish peroxidase (HRP) as a green species before the appearance of two already known red species during the HRP reaction.[1] This first compound (hence "Compound I") was later suggested to contain only one oxidizing equivalent (i.e., a monooxygen complex) based on reduction experiments with ferrocyanide in metmyoglobin[2] and HRP.[3,4] In the years to follow, cytochrome P450 enzymes (P450) were discovered[5,6] and the search for their reaction mechanism began. The finding that the oxidizing species in P450 was of mono-oxygen character by using oxygen surrogates[7−10] fueled the notion that the oxidizing compound was indeed Cpd I, as found in HRP. Supporting this notion, synthetic Cpd I made later was shown to have similar spectroscopic features as the active species of HRP, and to be capable of olefin epoxidation as in P450.[11] Cpd I has indeed been observed in the related heme-sulfur ligated chloroperoxidase (CPO),[12] but in P450 this species has so far been elusive and has not yet been detected in enzymatic turnovers. There is, however, indirect evidence for its existence,[13,14] although its oxidation state has been questioned[15] and coexistence with other active oxidizing species has been suggested.[16] Due to its similarity to P450, nitric oxide synthase (NOS) is also assumed to generate Cpd I, although the associated evidence is somewhat weaker than in P450.[17]

Due to its elusive nature, theoretical studies on Cpd I, and on P450 reaction mechanisms in general, have been able to contribute missing clues in this field (for a review, see ref 18). The ground state of Cpd I is known to be either a doublet or a quartet (almost degenerate in energy). The three singly occupied valence orbitals for these states are named π^*_{xz}, π^*_{yz} and a_{2u}; there are two electrons with parallel spin in the two π^* orbitals, and the third unpaired electron can have either α or β spin. In addition, there is a sextet state as well as other states with more complicated orbital configurations such as hepta-radical sextet states[19] and a PorFe(V)O state,[20] all with higher energies.[21] Figure 1 shows the shape of the most relevant valence orbitals of Cpd I.

Although these theoretical results come mostly from quantum mechanical (QM) calculations on simple gas-phase models, some of the results have been obtained also from combined quantum mechanical and molecular mechanical (QM/MM) calculations, which include the whole protein.[22−25] The latter have the advantage of enabling us to estimate the impact of the protein environment on the active site, something that small gas-phase QM models cannot do. QM/MM comparisons have been reported[23,25] between the Cpd I structures of different human P450 isoforms, which were found to be quite similar despite the different environments. However, the human 3A4 isozyme exhibited clear and systematic fluctuations in the

† Part of the "Sason S. Shaik Festschrift".

* Corresponding author. E-mail: sason@yfaat.ch.huji.ac.il.

‡ The Hebrew University of Jerusalem.

§ Current address: Université Pierre et Marie Curie-Paris 6, Laboratoire de Chimie Organique (UMR 7611 CNRS), Institut de Chimie Moléculaire (FR 2769), 4 Place Jussieu B. 229, 75005 Paris, France.

|| Max-Planck-Institut für Kohlenforschung.

10.1021/jp806770y CCC: $40.75
Published on Web 10/14/2008

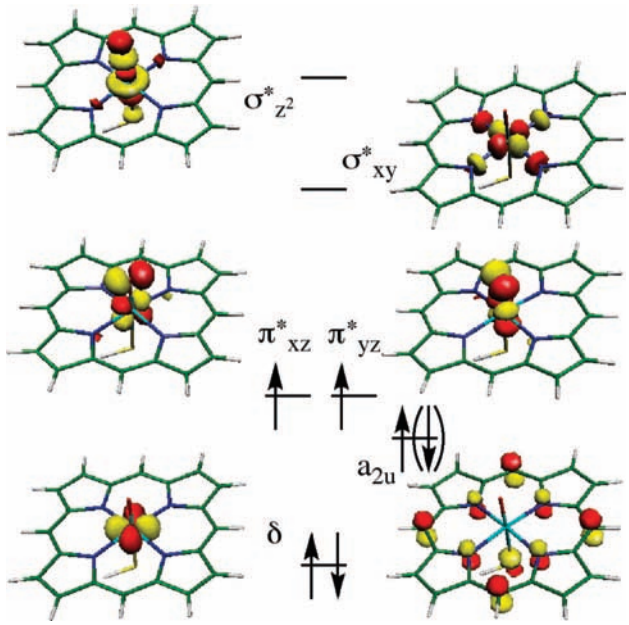

Figure 1. Valence orbitals of Cpd I. The arrows indicate the occupancy for the quartet (doublet) configuration.

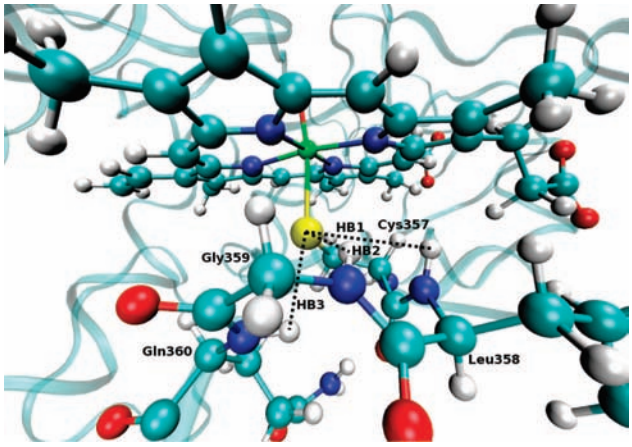

Figure 2. Three possible NH—S hydrogen bonds (denoted HB1, HB2 and HB3) to the heme-ligated cysteine sulfur in $P450_{wt}$ highlighted.

electronic structure as a function of the cooperative binding of two substrate molecules that controlled the proximity of one of them to the Fe═O moiety.[25] Furthermore, a recent QM/MM study of Cpd I of the bacterial isoform P450 StaP shows that in the presence of the native substrate, the a_{2u} electron can be delocalized toward the substrate.[26] Clearly, Cpd I can show significant variance, and it is important to determine the extent of this variance and its dependence on the environment and on the different residues/additives within a given protein.

For a more comprehensive assessment of the structures and other properties for Cpd I species of different heme enzymes, we have explored by QM/MM calculation the putative Cpd I species for four different heme-sulfur ligated enzymes, namely $P450_{cam}$ ($P450_{wt}$), the L358P mutant of $P450_{cam}$ (L358P), CPO and NOS. In addition, we have considered two snapshots from a molecular dynamics simulation of the L358P mutant, to investigate the range of fluctuations within a single enzyme. Also, L358P deserves a closer look as the mutation removes one of the potential NH---S hydrogen bonds on the proximal side of the heme (Figure 2), which should increase the "push" effect in the O—O cleavage step.[27,28] This mutant is also expected to mimic the wild-type structure with putidaredoxin bound, where heme reduction is facilitated.[29]

The QM/MM calculations were performed on each of the five enzyme models using three different QM model regions, and each of these model regions were calculated in both the doublet and quartet states, yielding thirty different structures. In addition, we also looked at the possibility of including a water molecule hydrogen-bonded to the iron-oxo moiety. If not present in a PDB file, this water molecule may be considered as a product of the O—O bond cleavage step during Cpd I formation. In the calculations, this water is either explicitly included in the QM region or absent altogether. This effectively doubles the number of structures considered, and we thus present here in this study 60 different structures calculated with QM/MM, in addition to four simple gas-phase QM models included for the sake of comparison. This computational investigation should thus allow us to assess the effects of the different protein environments on the properties of Cpd I. To the best of our knowledge, this is the first time heme thiolate enzymes have been compared to each other with QM/MM cross the enzyme boundaries.

Methods

Preparations for $P450_{wt}$. A detailed description of the setup of the $P450_{cam}$ system has been published elsewhere, see Supporting Information of ref 22. This also serves as a general blueprint for the other enzymes presented here. In short, structure 1DZ9 from RCSB Protein Data Bank was solvated in a 16 Å water layer, and the inner layer (<8 Å) was equilibrated for 3 ps at 300 K. The soaking and equilibration were repeated three times to get a reasonable solvent density. No MM minimization was done on the enzyme itself before the QM/MM calculations were started, and thus the enzyme heavy-atom coordinates correspond exactly to those from the starting PDB file. For the calculations without water hydrogen-bonded to Fe—O, the coordinates of crystal water 325 were deleted. Unlike in the previous study,[22] however, Asp297 was protonated, following insights gained later.[30,31]

Preparations for L358P. The published crystal structure of a ferrous-CO complex of the L358P mutant (PDB ID: 1T85)[32] was used to prepare a suitable initial structure for the present QM/MM calculations. Specifically, chain A, which contains a K^+ ion, was used. The protonation states of residues were essentially the same as in the previous $P450_{wt}$ calculations,[22] except that also here Asp297 was protonated. The charge of the total system was −9, but the overall negative charge is not expected to affect the relative energies of the systems of interest here as tested before on $P450_{cam}$ Cpd I as well as the pentacoordinated state.[31,33] After solvating the system, the inner-layer solvent molecules were equilibrated according to the previously reported procedure.[22] The resulting structure was used as one starting point ("$L358P_{0ps}$") for QM/MM calculations (after replacing CO by O_2). A second starting structure for QM/MM was generated by energy minimization of the ferrous—CO complex with the ABNR algorithm for 3600 steps, followed by a 500 ps MD simulation with a time step of 1 fs (keeping the heme, CO, Cy357, and camphor atoms fixed). The snapshot after 475 ps in the MD trajectory has no longer a hydrogen bond between the side chain of Gln360 and the carbonyl group of Cys357 (unlike the X-ray structure) and was therefore chosen as second initial structure for QM/MM calculations ("$L358P_{475ps}$"). Furthermore, to analyze the effect of a water molecule forming a hydrogen bond with the oxo moiety, we also prepared models with a water molecule added at the corresponding position occupied by W903 in $P450_{wt}$ Cpd I.[34]

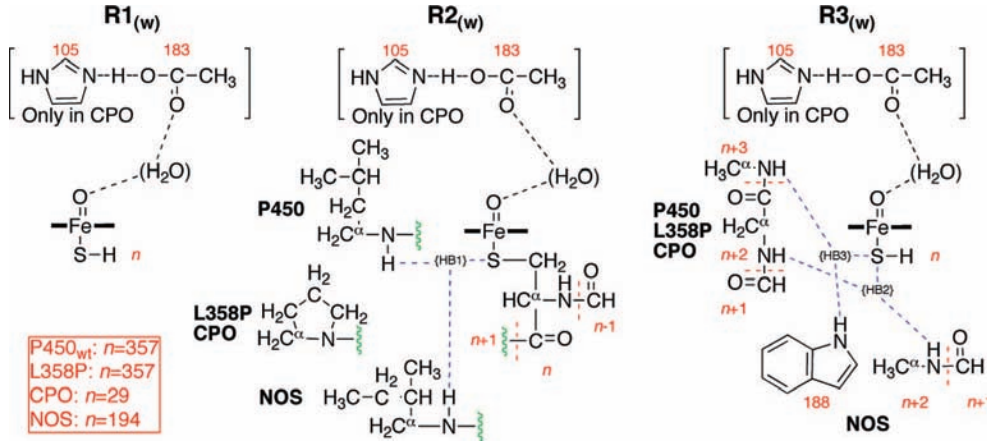

Figure 3. Schematic presentations of the three QM models (R1, R2 and R3) used in this study. If a water molecule is included, the model is designated with a subscript w (i.e., $R1_w$, $R2_w$ and $R3_w$). Red labels indicate the residue numbers in the different proteins, where *n* is the number of the cysteine ligand in the corresponding enzyme (see box in the lower left side). Blue dashed lines highlight the hydrogen bonds to sulfur as defined in Figure 2. The connecting points between the residues *n* and *n* + 1 are shown in green in the different enzymes.

For QM/MM calculations, we utilized the same CHARMM[35] topology/parameter sets as in the previous work on $P450_{wt}$ Cpd I.[22]

Preparations for CPO. To prepare suitable initial structures for QM/MM, we started from the experimental X-ray structure of Compound 0 (Cpd 0) of CPO (PDB ID: 2J5M) and modified it to build a complete Cpd I model of the solvated enzyme by adding and optimizing the missing hydrogen atoms as well as a 16 Å thick water solvent layer.[36] The total charge of the so-generated system was −16. Aspartic acid (Asp) and glutamic acid (Glu) residues were assumed to be ionized, i.e., negatively charged, and arginine (Arg) and lysine (Lys) residues were used as positively charged. The histidine residues were doubly protonated and hence each of them had one positive charge. There are two negative charges on the heme moiety, one negative charge on an acetate molecule near the pocket of the enzyme, and two positive charges on the Mn^{2+} ion coordinated to one of the propionate side chain of the protoporphyrin. In a recent QM/MM study of the formation of CPO Cpd I, we have tested the effect of the protonation state on the results by performing calculations on a neutral enzyme as well. The energetic results of the neutral enzyme were virtually the same (within 1.1 kcal/mol) as those for the −16 charged enzyme.[37] Here, the complete system consists of 18338 atoms, including 12735 atoms in the solvent. The inner solvent layer (<8 Å) was equilibrated for 3 ps at 300 K by performing pure force field energy minimizations and short molecular dynamics (MD) simulations, using the CHARMM22 force field.[35] The geometry obtained after MM minimization served as initial structure for the QM/MM calculations. For the QM model without the water hydrogen-bonded to the FeO moiety, we simply deleted this water from the PDB file. We used the CHARMM topology files for Cpd I[22] rather than those for Cpd 0.

Preparations for NOS. The published crystal structure (PDB ID: 1NOD)[38] was prepared according to the procedures described in previous QM/MM work on NOS.[39] In short, the crystal structure was supplemented with missing residues and O_2 followed by repeated soaking in a 16 Å layer of water, with short CHARMM molecular dynamics and minimization runs in between. Because the resulting structure is derived from the crystal structure without any extensive MD simulation, it is denoted as 0 ps snapshot. It was previously shown[39] that the addition of two protons resulted in Cpd I formation. Hence, even though the initial preparations were done on an O_2-bound heme structure, the earlier QM/MM calculations were performed by converting a H_2O_2-bound structure to the putative Cpd I structure; it is this structure that we have used in the current study (structure **3P** in ref 39). For the QM model without the water hydrogen-bonded to the FeO moiety, we again simply deleted this water from the PDB file. We employed the CHARMM topology files for Cpd I[22] (rather than those for the heme−O_2 complex). Also, because the addition of the two protons resulted in the conversion of the cofactor tetrahydrobiopterin to a cation radical species ($H_4B^{\bullet+}$), and this species is in the MM region in the present study, we adopted the H_4B parameters[39] and modified its overall charge from neutral to +1.

TABLE 1: Protein Sequence in the Immediate Vicinity of the Cysteine Ligand (Marked in Bold)

enzyme	protein sequence
$P450_{wt}$	Leu356, **Cys357**, Leu358, Gly359, Gln360
L358P	Leu356, **Cys357**, Pro358, Gly359, Gln360
CPO	Pro28, **Cys29**, Pro30, Ala31, Leu32
NOS	Arg193, **Cys194**, Ile195, Gly196, Arg197

QM Regions. For future reference, we define the hydrogen bonds to the ligated cysteine sulfur as HB1, HB2 and HB3 (see Figures 2 and 3). HB1 is the hydrogen bond to the backbone NH group of the residue *n* + 1, where *n* is the cysteine ligand residue number (e.g., Cys357 in $P450_{cam}$). HB2 is the hydrogen bond to the NH group of *n* + 2, and HB3, the bond to the NH of residue *n* + 3. In the case of NOS, HB3 is the hydrogen bond to Trp188 instead. Some of these hydrogen bonds will cross the QM and MM region boundary, depending on the QM model. Also, note that the "HB" designation primarily refers to the distances between the relevant atoms; whether or not these distances are actually real hydrogen bonds are discussed further below. Table 1 shows the relevant amino acid sequence numbers involved in the models.

In each of the enzymes, three different models were chosen. Figure 3 specifies the atoms included in the models for each of the enzymes.

R1: The model contains porphine as a heme model, with SH replacing the cysteine ligand.

R2: As for R1, but the cysteine ligand is now modeled by the full cysteine residue. Also included are the CO group of the previous residue as well as the atoms of the following residue up to the C^{α} atom (including the side chain).

R3: As for R1, but with addition of the nitrogen atoms hydrogen-bonded to sulfur that were not included in R2. The

backbone atoms of the protein, starting from the CO group in the residue after the cysteine ligand up to the C^{α} atom three residues thereafter, are included but without any side chains. In the case of NOS, sulfur forms the third hydrogen bond with the side chain of Trp188 instead, and therefore, only a $HCO-NH-C^{\alpha}H_3$ group representing the peptide bond of Gly196 and Arg197 is present, together with an indole ring representing Trp188. The extended models denoted as $R1_w$, $R2_w$ and $R3_w$ contain, in addition to R1, R2 and R3, also a water molecule hydrogen-bonded to the iron-oxo moiety. The gas-phase calculations were done only for the R1 models, with or without water ($R1_{(w)}$).

In the case of CPO, all models also include the side chains of His105 and Glu183. The reason for the inclusion of these distal residues in CPO is that CPO has a polar active site like other peroxidases, and the two nearest polar residues to heme are His105 and Glu183. Recent QM/MM mechanistic study has shown that they play an important role in Cpd I formation in CPO.[37] Also, because a proton is shared between these two residues, the complex is better modeled with QM rather than with MM.

QM/MM Calculations. QM/MM calculations[40] were performed with ChemShell 2.05b4[41] combining the QM capabilities of Turbomole 5.71[42] and the MM capabilities of the ChemShell built-in version of DL_POLY using electronic embedding.[43] The QM part was treated by density functional theory (DFT)[44] using the B3LYP hybrid functional,[45−48] shown to perform well in these particular systems compared to both experimental results[21,33,49,50] and ab initio MRCI-calculations.[24,51] During geometry optimizations, 6-31G basis set was used, except for iron (LACVP basis) and the O/N/S atoms ligated to iron (6-31+G*). This combination of basis sets is denoted as B2. Single-point calculations were done on the optimized geometries with a larger basis set to obtain more accurate energies and electronic properties. This basis set was composed of different basis sets depending on the atom types. On Fe, Wachters' all-electron basis was used including the two p-type polarization functions whose exponents were scaled by 1.5.[52] This basis set was augmented with a 3d diffuse function[53] and a set of contracted diffuse f-functions derived from a 3-term Gaussian expansion of an 4f STO orbital,[54] whose exponents were scaled with a factor of $3.6^2/3.6$ (GTO/STO), respectively.[55] The basis set was contracted as (8s7p4d1f), and the exponents and coefficients are provided in Supporting Information. The iron-ligated atoms O/N/S used 6-31+G*, and nitrogen atoms with hydrogen bonds to sulfur as well as for the oxygen atom in water (if present) used 6-31G*, and 6-31G was used for the rest. In CPO, 6-31+G* was also used for the nitrogen and oxygen atoms in the $-N\cdots H\cdots O_2C-$ hydrogen-bonded complex of His105 and Glu183. This larger basis set is denoted as B3. The MM part was treated with CHARMM22 potentials,[35] and the active-site region around the QM model that was allowed to relax is defined in the Supporting Information. Default ChemShell convergence criteria were used in all calculations.

Dipole Moments and Protein Electric Fields. To quantify and visualize the effect of the enzyme on the QM region, dipole moments and protein electric fields were computed for R1 models in the doublet spin states (^{2}R1), without water and using basis B3. The dipole moments were calculated for the QM region at the QM/MM optimized geometries using Turbomole. For the sake of comparison, the His105-Glu183 part of CPO was put into the MM region for these specific calculations. Two dipole moments were calculated at this geometry, one in the gas phase, and the other one with the MM charges included. The electric fields were evaluated using the built-in feature of ChemShell 3.1, for calculating the electric field generated by the MM charges at any position. We determined the electric fields at the location of iron and its six ligand atoms, and computed their average in magnitude and direction. For the purpose of visualization, this average field is associated with the position of the iron atom.

It should be noted that in ChemShell, the direction of the electric field is defined to point from + to − following the prevailing convention, and the dipole moment is normally defined to point from − to +. Despite the opposite definition of the dipole moment and the electrical field, they are not necessarily opposite to each other because they derive from different set of charges (QM and MM atoms, respectively). If the MM electric field vector and the QM dipole moment vector are properly aligned, Cpd I will be considered as being stabilized by the environment.

Mössbauer Calculations. Mössbauer parameters were determined by single-point calculations at optimized structures using the ORCA package.[56] The isomer shift δ was evaluated from the electron density at the iron nucleus.[57] Iron was described by the triply polarized core properties basis set CP(PPP)[57] and the other atoms by the SV(P) basis set[58] with the inner s-functions left uncontracted. For the iron atom, an enhanced integration grid was used and the overall integration accuracy was increased to 7.[57] MM point charges were included in these calculations to probe the effect of the protein environment. To decide which of the QM models to use for the Mössbauer calculations, experimental values for CPO[12] were taken as references in initial tests. In calculations on all doublet CPO structures, the $^2R3_{(w)}$ values showed the closest match with the experimental values (Table SK1, Supporting Information). The results for the ^{2}R3 (without water) structure showed a lower and less accurate quadrupole splitting (ΔE_q), but a higher isomer shift (δ) value, which was closer to the experimental values. As our trial runs indicate that ΔE_q is the most sensitive parameter, we decided to use the ^2R3_w structures in all enzymes for the Mössbauer evaluations. The Mössbauer parameters for the quartet structure ^4R3_w show negligible differences to those for ^2R3_w.

Results

Energies. Comparing the energies between the different multiplicities, it is clear that the doublet and quartet structures are close in all cases (Figure 4 and Table SK2, Supporting Information). This is a result known from previous individual calculations, and we confirm it here in a systematic way for a wide range of different QM regions as well as enzyme environments. Although the energies are close enough to be called degenerate, in the majority of cases the doublet state is slightly lower. The single largest energy difference between a doublet and corresponding quartet is 0.49 kcal/mol; the average energy difference is in fact only 0.10 kcal/mol (not including the gas-phase values). Thus Cpd I species may exist in both multiplicities and thereby give rise to two-state reactivity which may be observable experimentally, e.g., through differences in kinetic isotope effects[59] and other criteria, as amply discussed in the literature.[60−63]

The largest energy variations are seen in NOS. In fact, without taking NOS into account, the values of the single largest and average energy differences are only 0.15 and 0.04 kcal/mol, respectively. Thus, although the variations themselves are not

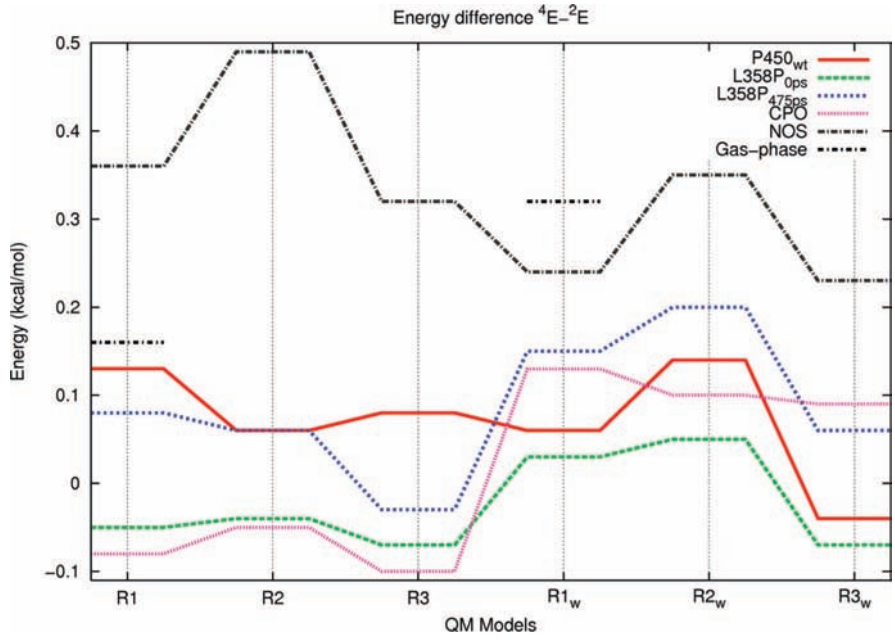

Figure 4. Relative energy difference E(quartet) − E(doublet) in kcal/mol for all six QM models.

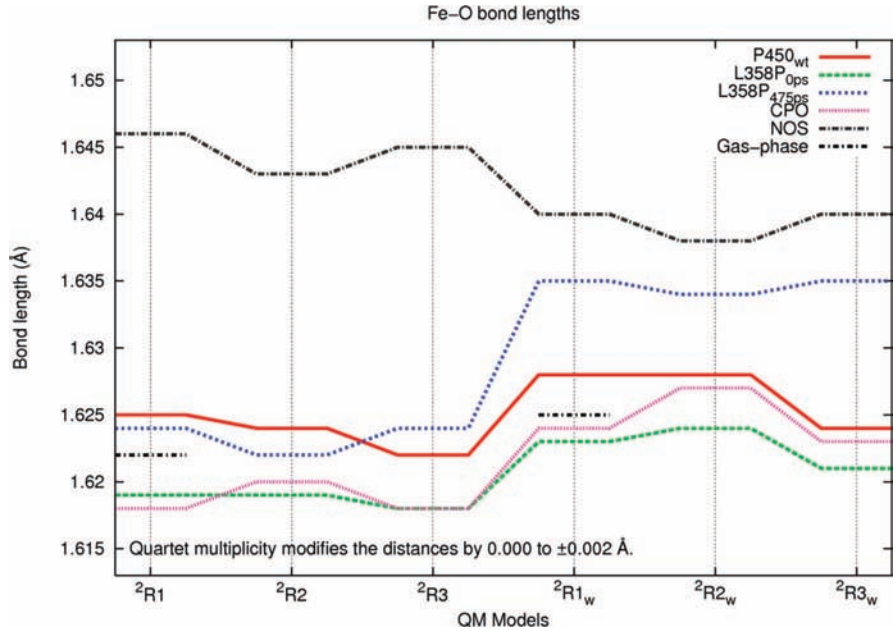

Figure 5. Doublet Fe−O distances in Å for all six QM models.

so large, the environment around NOS seems to favor slightly larger spin state splittings than in the other enzymes.

Geometries. The Cpd I structures are similar for all enzymes studied (Table SK4, Supporting Information). Most notably, the Fe−O distance remains between 1.62 and 1.65 Å regardless of multiplicity, QM region or presence of water (Figure 5). The longest Fe−O bonds are found in NOS with 1.64−1.65 Å, compared with 1.62−1.64 Å in the other enzymes. The insensitivity of the Fe−O bond is even more remarkable given that there may or may not be a water molecule hydrogen-bonded directly to the oxygen, and if there is, the hydrogen bonding distance to the water varies from 1.58 to 1.86 Å (Figure 6).

The Fe−S bond length shows a slightly larger variation (Figure 7). The shortest bond lengths are seen in the mutant $L358P_{0ps}$ structures (with water) as well as in the wild type, with values just below or around 2.50 Å. The largest bond lengths are found in the same enzyme in the 475 ps structure (almost 2.60 Å), as well as in NOS. The difference between the two L358P snapshots probably arises from the lack of hydrogen bonding between the backbone O of Cys357 and the side chain of Gln360 in the 475 ps snapshot and not from the different enzyme environment (see Discussion). It serves as a reminder, however, that one should not overemphasize small differences between different enzymes nor underestimate the fluctuations in a given enzyme due to statistical sampling. Nevertheless, a systematic trend, varying in magnitude, can be clearly seen in Figure 7 where the Fe−S bond becomes shorter in the water bound structures compared to their counterparts without water. This is true in all the enzymes and QM models and indicates that indeed the interactions with the Fe−O in the distal side of the heme have a consequence on the Fe−S bond in the proximal side.

In a previous study of the Cpd I geometry, it was observed that the Fe−S bond distance may become shorter by up to 0.1

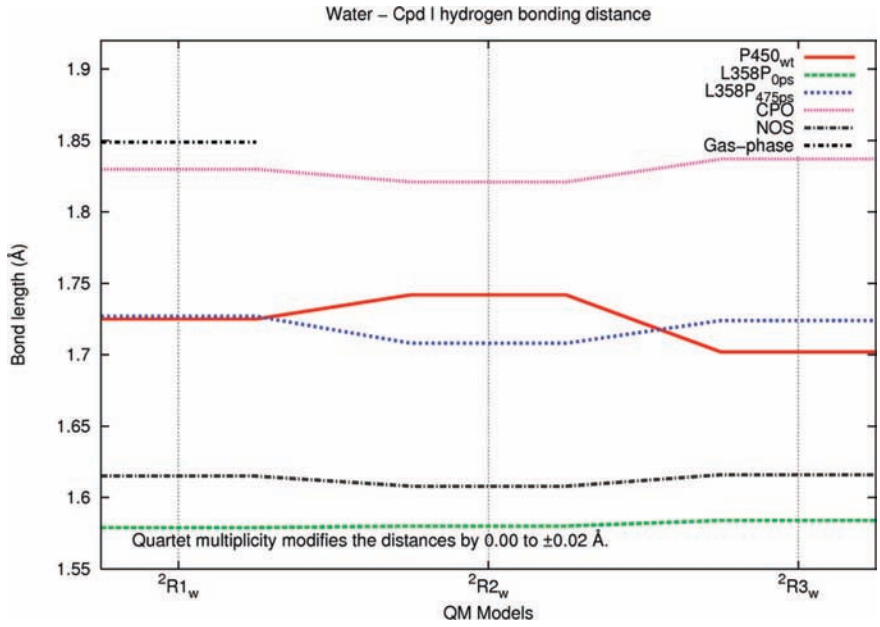

Figure 6. FeO — H_2O hydrogen bonding distances in Å for the three doublet QM models.

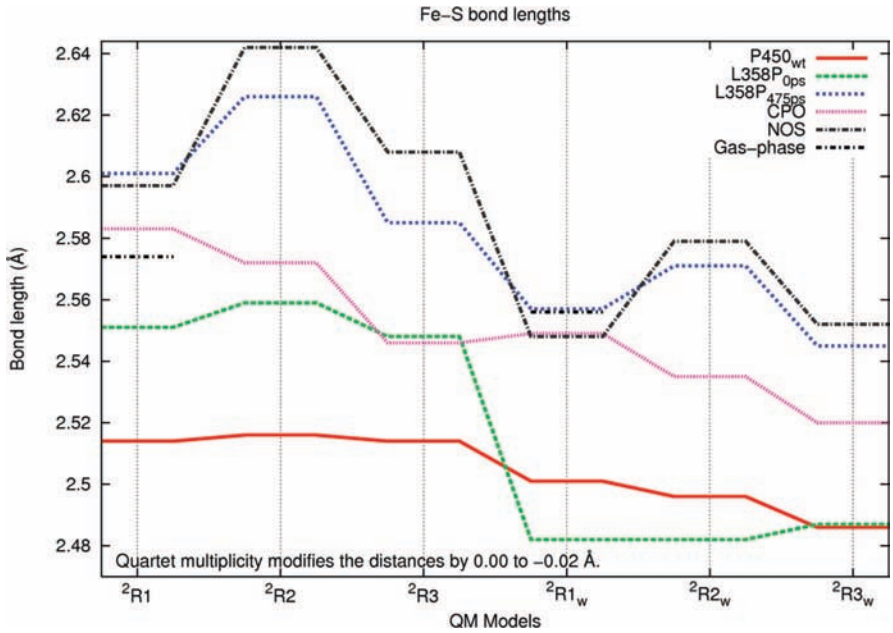

Figure 7. Doublet Fe−S distances in Å for all six QM models.

Å in the $P450_{wt}$ protein environment compared with that of the gas phase, depending on the basis set and the QM model.[22] However, for an R1 model, no shortening was observed in the chosen snapshot (29 ps). In the current study (with the 0 ps snapshot), a small shortening of about 0.05 Å is indeed seen in $P450_{wt}$ using the $R1_{(w)}$ models, and there is also a shortening in $L358P_{0ps}$ with water. In all the other $R1_{(w)}$ structures, however, the Fe−S bond length more or less retains its gas-phase value, suggesting again that HS− is a reasonable representation of the cysteine model in the gas-phase bare systems.[22] One feature that is clearly visible and not seen in the gas-phase models, however, is that in all the enzyme models, the porphine ring is nonplanar. This is due to porphyrin side-chain interactions with the protein that cause some strain. By contrast, the porphine ring system is unstrained and hence perfectly planar in the gas phase. The consequences of these geometry differences have already been discussed in the case of $P450_{wt}$.[22]

Hydrogen Bonds. To assess the strength of each of the relevant hydrogen bonds (see Methods),[64] we list in Table 2 the corresponding bond lengths and angles for ^2R2_w and ^2R3_w models (full listings in Table SK3, Supporting Information). In $P450_{wt}$, the HB1 bond length is not unreasonably long, but the small angle of less than 90° makes this interaction rather weak. This is largely true for HB1 in NOS as well, although the angle is somewhat more favorable. HB2 shows a stronger interaction with a short and more linear hydrogen bond arrangement, except for NOS. HB3 exhibits some variation, from a strong hydrogen bond in CPO to a very weak and distant interaction in the $L358P_{475ps}$ structure.

Spin Densities. Table 3 lists the spin distributions for the $R3_{(w)}$ structures, which are typical for the other models as well. According to Table 3, the combined Fe−O spin density is in the range 2.13 − 2.21 for the doublet and 2.00−2.05 for the quartet. Looking at the distribution between Fe and O, NOS

TABLE 2: Calculated Hydrogen Bond Distances and Angles in Cpd I Using $R2_w$ and $R3_w$ Doublet Models[a]

	^2R2_w		^2R3_w	
	r(NH−S)	∠NHS	r(NH−S)	∠NHS
$P450_{wt}$	3.37/2.43/2.93	85.3/139.5/103.0	3.38/2.49/2.94	85.8/139.7/105.3
$L358P_{0ps}$	----/2.39/2.81	----/140.6/109.4	----/2.45/2.96	----/137.0/108.0
$L358P_{475ps}$	----/2.43/3.85	----/148.6/97.4	----/2.44/3.89	----/146.7/98.9
CPO	----/2.60/2.42	----/145.0/174.5	----/2.61/2.45	----/141.3/173.0
NOS	3.16/3.26/2.63	126.2/94.0/139.4	3.52/3.21/2.59	119.1/95.9/145.3

[a] Values for HB1/HB2/HB3 in Å and degrees.

TABLE 3: Spin Densities for $R3_{(w)}$ Calculations ($R1_{(w)}$ for the Gas Phase) Using Basis B3

	without water					with water					
	ρ(Fe)	ρ(O)	ρ(Por)	ρ(S)	ρ(rest)	ρ(Fe)	ρ(O)	ρ(Por)	ρ(S)	$\rho(H_2O)$	ρ(rest)
					$P450_{wt}$						
doublet	1.30	0.88	−1.03	−0.16	0.00	1.37	0.81	−1.05	−0.14	0.01	0.00
quartet	1.15	0.87	0.86	0.12	0.00	1.21	0.80	0.87	0.11	0.01	0.00
					$L358P_{0ps}$						
doublet	1.31	0.88	−1.03	−0.15	0.00	1.40	0.76	−1.05	−0.13	0.02	0.00
quartet	1.15	0.87	0.85	0.13	0.00	1.26	0.75	0.87	0.10	0.02	0.00
					$L358P_{475ps}$						
doublet	1.33	0.87	−0.97	−0.23	0.00	1.45	0.75	−1.02	−0.19	0.01	0.00
quartet	1.14	0.86	0.80	0.20	0.00	1.26	0.74	0.83	0.15	0.01	0.00
					CPO						
doublet	1.25	0.92	−1.06	−0.09	−0.01	1.30	0.83	−0.99	−0.07	−0.06	−0.01
quartet	1.14	0.89	0.88	0.08	0.01	1.24	0.81	0.81	0.05	0.09	0.01
					NOS						
doublet	1.52	0.69	−0.80	−0.26	−0.15	1.51	0.68	−0.88	−0.20	0.01	−0.11
quartet	1.33	0.69	0.61	0.20	0.16	1.34	0.68	0.68	0.16	0.02	0.13
					Gas Phase						
doublet	1.29	0.86	−0.59	−0.58	0.02	1.34	0.80	−0.58	−0.58	0.01	0.02
quartet	1.15	0.88	0.46	0.52	−0.01	1.21	0.82	0.47	0.51	0.01	−0.01

stands out with highest spin density on Fe, 1.52/1.33 and 1.51/1.34 in the doublet/quartet without and with water, respectively. It is noteworthy that the water−Cpd I hydrogen bonding lowers the spin density on oxygen and raises it on iron (by about 0.1) in most of the enzymes while keeping the total FeO spin density constant, which indicates a modification of the π^* valence orbitals; NOS seems to be unaffected by this hydrogen bond. The spin density change brought about by hydrogen bonding to the iron−oxo moiety has been addressed before for the HRP enzyme and explained in terms of a simple valence bond model, whereby increasing the ionicity of the FeO bond is shown to cause an increase of spin on iron and a decrease on oxygen.[65]

The combined Por-S spin density ranges from −1.21/+0.81 to −1.06/+1.00 (doublet/quartet) without water; i.e., no large variations are seen. However, as noted before,[22] gas-phase Cpd I structures exhibit an evenly distributed sulfur−porphyrin radical, whereas in all the protein structures, most of this spin density is localized on the porphyrin ring (as have been observed experimentally in CPO[66]). It should be noted though that in NOS, unlike in other enzymes, there is some spin density in other parts of the QM region (Table 3). This is in fact only found in the R3 models, where the spin density on the Por-S moiety is lower by about 0.2 compared with the R1 and R2 models (Tables SG2 and SH2 in the Supporting Information). This amount of spin density is instead seen on Trp188 that is hydrogen-bonded to the sulfur in NOS. Hence, the a_{2u}-type orbital is delocalized not only over the Por-S moiety in NOS but also over Trp188.

Charge Distributions. Mulliken charges are known to be heavily dependent on the chosen basis set and model, so our analysis will focus on trends. As we are mainly concerned with the stabilization of the charge at sulfur in the presence or absence of HB1, we limit our comparisons to $R2_{(w)}$/B3 models (Table 4, other charges are available in the Supporting Information). Compared with $P450_{wt}$ the charge at sulfur is slightly more negative in $L358P_{0ps}$ (by about 0.03) and somewhat more positive in $L358P_{475ps}$ (by about 0.1). The most negative charge at sulfur is found in CPO, and the most positive one in NOS, with a difference of about 0.3 between these two extremes.

Mössbauer Parameters. The calculated Mössbauer parameters (see Methods for details) are given in Table 5, alongside values taken from other studies for the sake of comparison. The different values for the two snapshots of L358P show that the quadrupole splitting ΔE_q can vary somewhat in a given enzyme depending on the actual environment. The computed quadrupole splitting values increase in the sequence P450 < CPO < NOS, whereas the isomer shifts change less. The calculated and observed Mössbauer parameters for CPO are in reasonable agreement. Furthermore, comparison with the gas-phase values, calculated for a model that is slightly different from ours,[24] shows that the protein affects the quadruple coupling. The value for NOS being the closest to a gas-phase value is in accord with the larger spin density on the sulfur, which indicates that the protein environment of this enzyme has the smallest effect on the push effect of the thiolate among these enzymes.[67]

Electric Fields from the Enzyme. As can be seen in Figure 8, the protein electric fields of $P450_{wt}$, L358P and CPO are pointing in similar directions, roughly perpendicular to the plane of the heme, with $L358P_{475ps}$ deviating only slightly from the others. NOS is distinctly different, with the electric field being more parallel to the plane of the heme. The numerical

TABLE 4: Calculated Mulliken Charges for $R2_{(w)}$ Models Using Basis B3

	without water					with water					
	Q(Fe)	*Q*(O)	*Q*(Por)	*Q*(S)	*Q*(rest)	*Q*(Fe)	*Q*(O)	*Q*(Por)	*Q*(S)	*Q*(H_2O)	*Q*(rest)
					$P450_{wt}$						
doublet	1.31	−0.33	−0.34	−0.54	−0.09	1.34	−0.47	−0.35	−0.53	0.09	−0.08
quartet	1.31	−0.32	−0.35	−0.55	−0.09	1.34	−0.46	−0.35	−0.54	0.09	−0.08
					$L358P_{0ps}$						
doublet	1.36	−0.32	−0.41	−0.57	−0.06	1.39	−0.42	−0.49	−0.56	0.14	−0.05
quartet	1.36	−0.31	−0.40	−0.58	−0.06	1.38	−0.41	−0.49	−0.57	0.13	−0.05
					$L358P_{475ps}$						
doublet	1.31	−0.32	−0.50	−0.44	−0.05	1.27	−0.45	−0.44	−0.43	0.09	−0.04
quartet	1.30	−0.32	−0.49	−0.45	−0.05	1.27	−0.44	−0.43	−0.44	0.09	−0.05
					CPO						
doublet	1.31	−0.26	−0.37	−0.67	−0.02	1.32	−0.41	−0.41	−0.68	0.22	−0.03
quartet	1.31	−0.26	−0.37	−0.67	−0.02	1.32	−0.41	−0.41	−0.68	0.22	−0.03
					NOS						
doublet	1.38	−0.65	−0.36	−0.35	−0.02	1.30	−0.52	−0.48	−0.35	0.06	−0.01
quartet	1.37	−0.64	−0.36	−0.35	−0.02	1.30	−0.51	−0.48	−0.36	0.06	−0.01

TABLE 5: Calculated Mössbauer Parameters (^2R3_w Models), Values from Other Theoretical Studies and Experimental Data for CPO

	η	ΔE_Q (mm/s)	δ (mm/s)
$P450_{wt}$	0.19	0.58	0.10
$P450_{wt}$[a]	0.09	0.67	0.13
$P450_{wt}$(g)[b]	0.06	1.34	0.09
$L358P_{0ps}$	0.09	0.65	0.12
$L358P_{475ps}$	0.07	0.80	0.12
CPO	0.32	0.73	0.11
NOS	0.21	1.00	0.08
NOS[c]	0.20	1.29	0.09
CPO exp[d]	n/a	1.02	0.15

[a] Values from ref 24 (in protein). [b] Gas-phase values from ref 24. [c] Values from ref 39. [d] Values from ref 12.

results for the electric fields are tabulated in Table SK5, Supporting Information.

It is obvious from Figure 8 that the intrinsic dipoles of the QM region of the various Cpd I species are relatively small (white arrows). They depend on the porphyrin geometry. In the gas-phase structures with a planar porphyrin, the dipole moment is pointing "down" toward the proximal side of the heme plane, whereas in all currently studied enzymes, the dipole moment is reversed. This dipole flip is in fact not surprising considering the magnitude of the dipole, which for the gas-phase dipole moment is 0.2815 au (Table SK6, Supporting Information). This corresponds to, for instance, two point charge centers with ± 5 in elementary charge separated by a distance of 0.03 Å (the larger charge, the smaller distance). It is therefore entirely plausible that rather small heme-plane distortions upon placement in an enzyme environment can shift the location of the positive and/or negative charge centers, causing a change in the direction of the dipole moment. The external electric field of the protein from the MM charges (blue arrows) polarizes the QM region and reinforces the dipole moments (red arrows). This is in accord with the changes in the spin density on the sulfur and porphyrin moieties. The numerical results for the dipole moments are tabulated in Table SK6, Supporting Information.

Comparisons to Known Experimental Values. Due to the transient nature of Cpd I, experimental information about this species remains scarce. However, there are some studies that do provide some information for comparison, mostly on CPO. The results from an early Mössbauer study[12] on CPO Cpd I are in reasonable agreement with the calculated Mössbauer parameters (Table 5) although there is room for improvement. A rapid freeze-quench ENDOR study[66] of the same species estimates an upper limit of 0.23 for the spin density on the sulfur ligand, a value exceeded only by $L358P_{475ps}$ and NOS in this study. X-ray absorption spectroscopy on CPO[68] gives an Fe−O distance of 1.65 Å and an Fe−S distance of 2.48, both values in reasonable agreement with our results. It is also interesting to note that X-ray diffraction data for $P450_{wt}$[34] indicate an Fe−O distance around 1.65 Å in the active species, which has, however, not been conclusively characterized; nevertheless, this value is close to our present results.

Discussion

All in all, the DFT calculations show that the Cpd I geometries do not vary much in the different enzymes. For instance, if the Fe−O bond length can be taken as an indication of the Fe−O bond strength, one can conclude that it is remarkably insensitive to the environment, as already noted before.[22,23] This is probably because the Fe−O bond is relatively strong (formally a double bond). Limiting the discussion to $P450_{wt}$, L358P and CPO, it is not surprising that the results are quite similar, given that the immediate coordination environment around the heme is often described as "identical". This is confirmed by analyzing the electric field around the active site generated by the MM charges, which is again similar for the three enzymes (blue lines, Figure 8).

It is therefore interesting to note the differences between the two snapshots of L358P, particular with regard to the Fe−S bond distance and the spin density on sulfur. Clearly, as noted already for the human 3A4 isozyme,[25] this suggests that there is some flexibility in the sulfur ligation in this heme protein during its natural fluctuations. As the 475 ps snapshot was selected for its lack of hydrogen bonding between the backbone O of Cys357 and the side-chain of Gln360, it may well be that the differences to the 0 ps snapshot are caused by this missing hydrogen bond. The electric fields calculated in the present study indeed show only small variations due to the general enzyme environment (Figure 8), and therefore they presumably play only a minor role in differentiating the QM regions of these two snapshots.

The present results are in line with most earlier QM/MM comparisons between Cpd I species in different isoforms of human P450 enzymes[23] where no significant changes in the

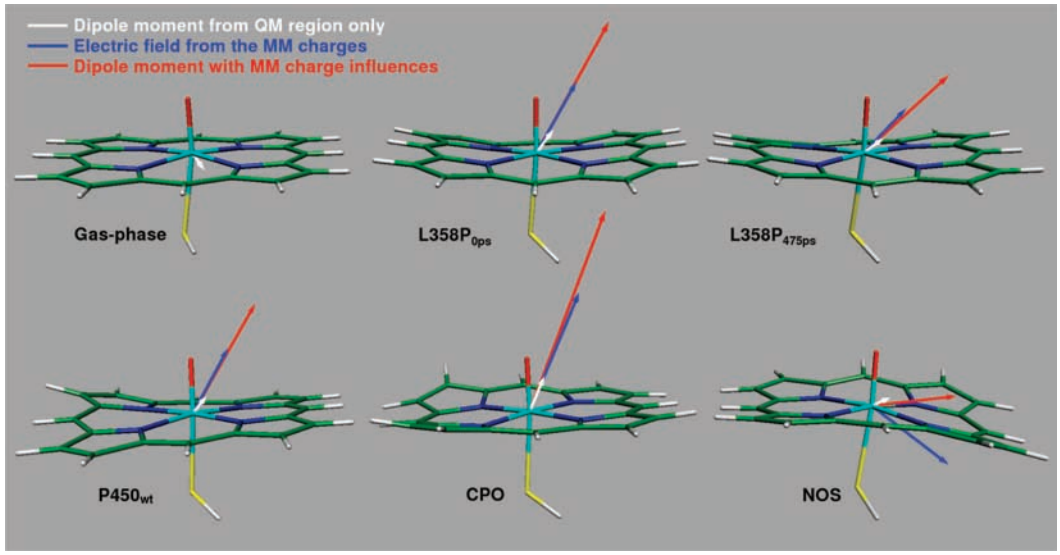

Figure 8. Calculated dipole moment and electric field vectors. The dipole moments are computed for the QM region at the QM/MM optimized geometries. This was done either without (white) or with (red) the MM point charges included. The relative magnitudes of these arrows are proportional to each other. The electric fields (blue) were calculated at iron and its six ligand atoms, and then averaged (see Methods).

electronic structure of Cpd I were seen for a wide variety of model parameters (heme substituents, thiolate representation, DFT functionals, protonation states of nearby residues, presence/absence of the substrate, etc.). As in the present case, the differences that were observed among different isoforms were not larger than those among different snapshots of the same isoform.[23]

The small difference between $P450_{wt}$ and L358P may indicate that the one missing hydrogen bond in the mutant may be less important. L358P is designed to remove one putative hydrogen bond between $P450_{wt}$ Leu358 backbone NH and the proximal ligand sulfur (HB1), which has been proposed to increase the "push"-effect of the cysteine ligand and thus to facilitate O−O cleavage during Cpd I formation.[27] Though the presence of HB1 may influence this reaction, we do not find any evidence in this study that the mutation significantly affects any of the properties of Cpd I.

In fact, an analysis of a number of P450 PDB structures as well as theoretical calculations, past and current (Table 2), indicate that this distance (HB1) may not be of a hydrogen bonding character to start with, because of unsuitable N−H−S angles. In light of this, it would not be surprising that the removal of this interaction in L358P has little effect on the Cpd I structure. Comparison of the Mulliken charges on sulfur confirms that in the R2 model (which should be the most relevant one), they are comparable in $P450_{wt}$ and $L358P_{0ps}$, whereas $L358P_{475ps}$ shows about 0.1 less negative charge (see Supporting Information). The latter finding could be a secondary effect of the missing hydrogen bond in the 475 ps snapshot (see above); increased σ-electron donation from sulfur to the porphyrin was indeed observed in the Q360L mutant where this hydrogen bond is absent,[69] consistent with a shift of negative charge from sulfur to the porphyrin.

Bringing NOS into the discussion, it can be seen that NOS is quite different from the other investigated enzymes in several aspects. For example, the Fe−S bonds are among the longest in our study, the spin density on sulfur can only be compared to $L358P_{475ps}$, and the Mössbauer parameters are the closest to the gas phase. Even the otherwise so stable Fe−O bond is 0.01−0.02 Å longer than usual. Electric field calculations show that the influence of the enzyme on the heme is indeed different in NOS (and to a lesser extent, in $L358P_{475ps}$, Figure 8) and provide a partial explanation for these deviations. Our results are fully compatible with earlier gas-phase model calculations with external electric fields applied.[70] There, it was found that an external field along the S−Fe−O axis perpendicular to the heme plane affects the spin and charge distributions between the sulfur and the porphyrin, depending on the direction of the field. In contrast, the field parallel to the plane only affects the charge distribution within the porphyrin. From the Supporting Information one can also deduce that the energy differences between doublet and quartet Cpd I in the perpendicular field are larger than in the case of parallel or no field. Taking into account that the definition of the electric field direction is opposite to the one in the software used previously,[70] the trends in the energies and in the spin and charge distributions are all reproduced in the current study when comparing NOS (small electric field vector component in the S−Fe−O direction) with the other enzymes (large electric field vector component in the S−Fe−O direction).

Interestingly, in the R3 models of NOS, a small spin development is seen on Trp188 that is hydrogen-bonded to sulfur, whereas the spin density on the Por-S moiety is lowered by the same amount. This indicates a potential partial electron donor role of Trp188 (similar to CcP[71]) that invites further studies. Mutation studies with W409Y and W409F (where W409 is the corresponding residue in nNOS) have shown slower heme reduction in the mutants, but a faster decoupling of the self-regulatory heme−NO complex formed at the end of the NO synthesis.[71−73]

Concerning the Mössbauer parameters, Table 5 shows that the calculated values are, by and large, pretty similar and vary depending on the QM models used (Table 5 and Table SK1, Supporting Information). Previous gas-phase studies on ^{57}Fe Mössbauer parameters have provided estimated standard deviations of 0.18 mm s^{-1} for the quadrupole coupling[74,75] and 0.1 mm s^{-1} for the isomer shift[57,76] in such calculations. The current results for CPO are thus within the expected margin for the isomer shift, and somewhat beyond (too low) for the quadrupole splitting. Trends should be predicted quite reliably. Here, we expect that the isomer shifts will be similar to the CPO value for all the enzymes studied. For the quadrupole splitting, $P450_{wt}$

and NOS should be on opposite sides of the CPO value, whereas L358P should be close to CPO. Comparing with other theoretical work, our $P450_{wt}$ values are in line with previous QM/MM values (0.67, 0.09, and 0.13 for ΔE_q, η, and δ, respectively).[24]

Conclusions

The QM/MM studies show that the properties of Cpd I are changed significantly by the protein compared with the gas-phase situation. However, the Cpd I species in the four enzymes investigated here are overall similar, although some notable differences that do exist should not be overlooked. According to the QM/MM results, the more stable Cpd I in CPO should be a reasonably good model for the $P450_{wt}$ equivalent. Removal of the HB1 interaction in $P450_{wt}$ does not seem to have any large effect on the properties of Cpd I, indicating that other factors may be more important in the corresponding mutant L358P. However, the hydrogen bonding between water and the iron-oxo moiety in Cpd I alters the internal Fe−O spin distribution slightly in favor of less radical oxygen character (concomitant with some Fe−S bond shortening). This hydrogen bonding was recently shown to enhance the reactivity of Cpd I during camphor hydroxylation through electrostatic transition state stabilization.[77]

Among the four heme enzymes investigated presently, NOS deviates most from the others. This can be attributed to the more pronounced differences in the protein environment (e.g., reflected in the rather different electric fields generated at the heme site by the enzyme). This finding and the effects of substrates on the electronic and geometric structures of Cpd I in the human 3A4 isozyme of P450[25] and the bacterial enzyme P450 StaP[26] highlight the notion that the electronic structure of the Por(+•)FeO is mutable and susceptible to perturbation.[70] The changes in the present study are not large per se, but they are systematic and therefore of potential importance. The example of the catalytic water molecule in $P450_{cam}$ shows that such small perturbations may have a strong influence on the reactivity.[77] The drastic effect of the substrate that converts P450 StaP to a peroxidase-like enzyme[26] is another example of this mutability.

Acknowledgment. S.S. acknowledges support of an Israeli Science Foundation grant (ISF 16/06). H.H. is a JSPS postdoctoral fellow for research abroad, H.C. thanks the Golda Meir fellowship fund, and M.A.C. is supported by Generalitat de Catalunya.

Supporting Information Available: Calculated properties from the QM/MM calculations. This material is available free of charge via the Internet at http://pubs.acs.org.

References and Notes

(1) Theorell, H. *Enzymologia* **1942**, *10*, 250.
(2) George, P.; Irvine, D. H. *Nature* **1951**, *168*, 164.
(3) George, P. *Nature* **1952**, *169*, 612.
(4) George, P. *J. Biol. Chem.* **1953**, *201*, 413.
(5) Mason, H. S.; Fowlks, W. L.; Peterson, E. *J. Am. Chem. Soc.* **1955**, *77*, 2914.
(6) Hayaishi, O.; Katagiri, M.; Rothberg, S. *J. Am. Chem. Soc.* **1955**, *77*, 5450.
(7) Hrycay, E. G.; Gustafsson, J.-Å.; Ingelman-Sundberg, M.; Ernster, L. *FEBS Lett.* **1975**, *56*, 161.
(8) Hrycay, E. G.; Gustafsson, J.-Å.; Ingelman-Sundberg, M.; Ernster, L. *Biochem. Biophys. Res. Commun.* **1975**, *66*, 209.
(9) Lichtenberger, F.; Nastainczyk, W.; Ullrich, V. *Biochem. Biophys. Res. Commun.* **1976**, *70*, 939.
(10) Gustafsson, J.-Å.; Bergman, J. *FEBS Lett.* **1976**, *70*, 276.
(11) Groves, J. T.; Haushalter, R. C.; Nakamura, M.; Nemo, T. E.; Evans, B. J. *J. Am. Chem. Soc.* **1981**, *103*, 2884.
(12) Rutter, R.; Hager, L. P.; Dhonau, H.; Hendrich, M.; Valentine, M.; Debrunner, P. G. *Biochemistry* **1984**, *23*, 6809.
(13) Spolitak, T.; Dawson, J. H.; Ballou, D. P. *J. Biol. Chem.* **2005**, *280*, 20300.
(14) Dowers, T. S.; Rock, D. A.; Jones, J. P. *J. Am. Chem. Soc.* **2004**, *126*, 8868.
(15) Newcomb, M.; Zhang, R.; Chandrasena, R. E. P.; Halgrimson, J. A.; Horner, J. H.; Makris, T. M.; Sligar, S. G. *J. Am. Chem. Soc.* **2006**, *128*, 4580.
(16) Jin, S.; Bryson, T. A.; Dawson, J. H. *J. Biol. Inorg. Chem.* **2004**, *9*, 644.
(17) Stuehr, D. J. *Biochim. Biophys. Acta* **1999**, *1411*, 217.
(18) Shaik, S.; Kumar, D.; de Visser, S. P.; Altun, A.; Thiel, W. *Chem. Rev.* **2005**, *105*, 2279.
(19) Hirao, H.; Kumar, D.; Thiel, W.; Shaik, S. *J. Am. Chem. Soc.* **2005**, *127*, 13007.
(20) Ogliaro, F.; de Visser, S. P.; Groves, J. T.; Shaik, S. *Angew. Chem. Int. Ed.* **2001**, *40*, 2874.
(21) Altun, A.; Shaik, S.; Thiel, W. *J. Am. Chem. Soc.* **2007**, *129*, 8978.
(22) Schöneboom, J. C.; Lin, H.; Reuter, N.; Thiel, W.; Cohen, S.; Ogliaro, F.; Shaik, S. *J. Am. Chem. Soc.* **2002**, *124*, 8142.
(23) Bathelt, C. M.; Zurek, J.; Mulholland, A. J.; Harvey, J. N. *J. Am. Chem. Soc.* **2005**, *127*, 12900.
(24) Schöneboom, J. C.; Neese, F.; Thiel, W. *J. Am. Chem. Soc.* **2005**, *127*, 5840.
(25) Fishelovitch, D.; Hazan, C.; Hirao, H.; Wolfson, H. J.; Nussinov, R.; Shaik, S. *J. Phys. Chem. B* **2007**, *111*, 13822.
(26) Wang, Y.; Hirao, H.; Chen, H.; Onaka, H.; Nagano, S.; Shaik, S. *J. Am. Chem. Soc.* **2008**, *130*, 7170.
(27) Yoshioka, S.; Takahashi, S.; Ishimori, K.; Morishima, I. *J. Inorg. Biochem.* **2000**, *81*, 141.
(28) Ogliaro, F.; de Visser, S. P.; Shaik, S. *J. Inorg. Biochem.* **2002**, *91*, 554.
(29) Tosha, T.; Yoshioka, S.; Ishimori, K.; Morishima, I. *J. Biol. Chem.* **2004**, *279*, 42836.
(30) Zheng, J.; Altun, A.; Thiel, W. *J. Comput. Chem.* **2007**, *28*, 2147.
(31) Altun, A.; Shaik, S.; Thiel, W. *J. Comput. Chem.* **2006**, *27*, 1324.
(32) Nagano, S.; Tosha, T.; Ishimori, K.; Morishima, I.; Poulos, T. L. *J. Biol. Chem.* **2004**, *279*, 42844.
(33) Altun, A.; Thiel, W. *J. Phys. Chem. B* **2005**, *109*, 1268.
(34) Schlichting, I.; Berendzen, J.; Chu, K.; Stock, A. M.; Maves, S. A.; Benson, D. E.; Sweet, R. M.; Ringe, D.; Petsko, G. A.; Sligar, S. G. *Science* **2000**, *287*, 1615.
(35) MacKerell, A. D., Jr.; Bashford, D.; Bellott, M.; Dunbrack, R. L., Jr.; Evanseck, J. D.; Field, M. J.; Fischer, S.; Gao, J.; Guo, H.; Ha, S.; Joseph-McCarthy, D.; Kuchnir, L.; Kuczera, K.; Lau, F. T. K.; Mattos, C.; Michnick, S.; Ngo, T.; Nguyen, D. T.; Prodhom, B.; Reiher, W. E., III; Roux, B.; Schlenkrich, M.; Smith, J. C.; Stote, R.; Straub, J.; Watanabe, M.; Wiorkiewicz-Kuczera, J.; Yin, D.; Karplus, M. *J. Phys. Chem. B* **1998**, *102*, 3586.
(36) Kühnel, K.; Derat, E.; Terner, J.; Shaik, S.; Schlichting, I. *Proc. Natl. Acad. Sci. U.S.A.* **2007**, *104*, 99.
(37) Chen, H.; Hirao, H.; Derat, E.; Schlichting, I.; Shaik, S. *J. Phys. Chem. B.* **2008**, *112*, 9490.
(38) Crane, B. R.; Arvai, A. S.; Ghosh, D. K.; Wu, C.; Getzoff, E. D.; Stuehr, D. J.; Tainer, J. A. *Science* **1998**, *279*, 2121.
(39) Cho, K.-B.; Derat, E.; Shaik, S. *J. Am. Chem. Soc.* **2007**, *129*, 3182.
(40) Senn, H. M.; Thiel, W. *Top. Curr. Chem.* **2007**, *268*, 173.
(41) Sherwood, P.; de Vries, A. H.; Guest, M. F.; Schreckenbach, G.; Catlow, C. R. A.; French, S. A.; Sokol, A. A.; Bromley, S. T.; Thiel, W.; Turner, A. J.; Billeter, S.; Terstegen, F.; Thiel, S.; Kendrick, J.; Rogers, S. C.; Casci, J.; Watson, M.; King, F.; Karlsen, E.; Sjøvoll, M.; Fahmi, A.; Schäfer, A.; Lennartz, C. *J. Mol. Struct. (THEOCHEM)* **2003**, *632*, 1.
(42) Ahlrichs, R.; Bär, M.; Häser, M.; Horn, H.; Kölmel, C. *Chem. Phys. Lett.* **1989**, *162*, 165.
(43) Bakowies, D.; Thiel, W. *J. Phys. Chem.* **1996**, *100*, 10580.
(44) Kohn, W.; Sham, L. J. *Phys. Rev.* **1965**, *A140*, 1133.
(45) Becke, A. D. *Phys. Rev. A* **1988**, *38*, 3098.
(46) Becke, A. D. *J. Chem. Phys.* **1993**, *98*, 1372.
(47) Becke, A. D. *J. Chem. Phys.* **1993**, *98*, 5648.
(48) Lee, C.; Yang, W.; Parr, R. G. *Phys. Rev. B* **1988**, *37*, 785.
(49) Schöneboom, J. C.; Thiel, W. *J. Phys. Chem. B* **2004**, *108*, 7468.
(50) Wang, D.; Thiel, W. *J. Mol. Struct. (THEOCHEM)*, in press (DOI: 10/1016/j.theochem.2008.06.011).
(51) Altun, A.; Kumar, D.; Neese, F.; Thiel, W. *J. Phys. Chem. A*, in press.
(52) Wachters, A. J. H. *J. Chem. Phys.* **1970**, *52*, 1033.
(53) Hay, P. J. *J. Chem. Phys.* **1977**, *66*, 4377.
(54) Bauschlicher, C. W., Jr.; Langhoff, S. R.; Partridge, H.; Barnes, L. A. *J. Chem. Phys.* **1989**, *91*, 2399.
(55) Stewart, R. F. *J. Chem. Phys.* **1970**, *52*, 431.
(56) Neese, F. *ORCA Version 2.6 Revision 04*; University of Bonn: Bonn, Germany, 2006.

(57) Neese, F. *Inorg. Chim. Acta* **2002**, *337*, 181.
(58) Schäfer, A.; Horn, H.; Ahlrichs, R. J. *J. Chem. Phys.* **1992**, *97*, 2571.
(59) Cho, K.-B.; Moreau, Y.; Kumar, D.; Rock, D. A.; Jones, J. P.; Shaik, S. *Chem. Eur. J.* **2007**, *13*, 4103.
(60) Shaik, S.; Hirao, H.; Kumar, D. *Acc. Chem. Res.* **2007**, *40*, 532.
(61) Shaik, S.; Cohen, S.; de Visser, S. P.; Ogliaro, F.; Sharma, P. K. *Eur. J. Inorg. Chem.* **2004**, 207.
(62) Shaik, S.; Hirao, H.; Kumar, D. *Nat. Prod. Rep.* **2007**, *24*, 533.
(63) Shaik, S.; Ogliaro, F.; de Visser, S. P.; Schwarz, H.; Schröder, D. *Curr. Opin. Chem. Biol.* **2002**, *6*, 556.
(64) Poulos, T. L. *J. Biol. Inorg. Chem.* **1996**, *1*, 356.
(65) Derat, E.; Cohen, S.; Shaik, S.; Altun, A.; Thiel, W. *J. Am. Chem. Soc.* **2005**, *127*, 13611.
(66) Kim, S. H.; Perera, R.; Hager, L. P.; Dawson, J. H.; Hoffman, B. M. *J. Am. Chem. Soc.* **2006**, *128*, 5598.
(67) Cohen, S.; Kumar, D.; Shaik, S. *J. Am. Chem. Soc.* **2006**, *128*, 2649.
(68) Stone, K. L.; Behan, R. K.; Green, M. T. *Proc. Natl. Acad. Sci. U.S.A.* **2005**, *102*, 16563.
(69) Yoshioka, S.; Tosha, T.; Takahashi, S.; Ishimori, K.; Hori, H.; Morishima, I. *J. Am. Chem. Soc.* **2002**, *124*, 14571.
(70) Shaik, S.; de Visser, S. P.; Kumar, D. *J. Am. Chem. Soc.* **2004**, *126*, 11746.
(71) Poulos, T. L. *Nat. Prod. Rep.* **2007**, *24*, 504.
(72) Adak, S.; Crooks, C.; Wang, Q.; Crane, B. R.; Tainer, J. A.; Getzoff, E. D.; Stuehr, D. J. *J. Biol. Chem.* **1999**, *274*, 26907.
(73) Adak, S.; Wang, Q.; Stuehr, D. J. *J. Biol. Chem.* **2000**, *275*, 17434.
(74) Havlin, R. H.; Godbout, N.; Salzmann, R.; Wojdelski, M.; Arnold, W.; Schulz, C. E.; Oldfield, E. *J. Am. Chem. Soc.* **1998**, *120*, 3144.
(75) Godbout, N.; Havlin, R.; Salzmann, R.; Debrunner, P. G.; Oldfield, E. *J. Phys. Chem. A* **1998**, *102*, 2342.
(76) Zhang, Y.; Mao, J.; Oldfield, E. *J. Am. Chem. Soc.* **2002**, *124*, 7829.
(77) Altun, A.; Friesner, R. A.; Guallar, V.; Shaik, S.; Thiel, W. *J. Am. Chem. Soc.* **2006**, *128*, 3924.

JP806770Y